NWC TP 5726

Physicochemical Details at the Surface of Burning Illumination Flares

by
J. L. Eisel
and
D. E. Zurn
Research Department

APRIL 1975

Naval Weapons Center
CHINA LAKE, CALIFORNIA 93555

Naval Weapons Center

AN ACTIVITY OF THE NAVAL MATERIAL COMMAND

R. G. Freeman, III, RAdm., USN . . . . . Commander
G. L. Hollingsworth . . . . . Technical Director

FOREWORD

This report presents the results of a study of the combustion processes of pyrotechnic materials. The effects of metal content ratio, metal particle size, binder type, and binder content on the processes occurring at the burning flare surface are reported, as well as the concomitant changes in burning rate, intensity, and efficiency.

The work was supported by AIR TASK A350-350F/008B/3F54546000.

This report is prepared for timely distribution of information and may be subjected to modification as the result of continued research.

Released by
R. L. Derr, *Head*
Aerothermochemistry Division
8 April 1975

Under authority of
Hugh W. Hunter, *Head*
Research Department

NWC Technical Publication 5726

Published by . . . . . Research Department
Collation . . . . . Cover, 9 leaves
First printing . . . . . 200 unnumbered copies

UNCLASSIFIED

SECURITY CLASSIFICATION OF THIS PAGE *(When Data Entered)*

REPORT DOCUMENTATION PAGE		READ INSTRUCTIONS BEFORE COMPLETING FORM
1. REPORT NUMBER NWC TP 5726	2. GOVT ACCESSION NO.	3. RECIPIENT'S CATALOG NUMBER
4. TITLE *(and Subtitle)* Physicochemical Details at the Surface of Burning Illumination Flares		5. TYPE OF REPORT & PERIOD COVERED 1 Jul 1973 - 31 Dec 1974 Ongoing Research
		6. PERFORMING ORG. REPORT NUMBER
7. AUTHOR(s) J. L. Eisel and D. E. Zurn		8. CONTRACT OR GRANT NUMBER(s)
9. PERFORMING ORGANIZATION NAME AND ADDRESS Naval Weapons Center China Lake, CA 93555		10. PROGRAM ELEMENT, PROJECT, TASK AREA & WORK UNIT NUMBERS AirTask A350-350F/008B/ 3F54546000
11. CONTROLLING OFFICE NAME AND ADDRESS		12. REPORT DATE April 1975
		13. NUMBER OF PAGES 16
14. MONITORING AGENCY NAME & ADDRESS*(if different from Controlling Office)*		15. SECURITY CLASS. *(of this report)* Unclassified
		15a. DECLASSIFICATION/DOWNGRADING SCHEDULE
16. DISTRIBUTION STATEMENT *(of this Report)* Approved for public release; distribution unlimited		
17. DISTRIBUTION STATEMENT *(of the abstract entered in Block 20, if different from Report)*		
18. SUPPLEMENTARY NOTES		
19. KEY WORDS *(Continue on reverse side if necessary and identify by block number)* Flares, Pyrotechnics, Magnesium, Combustion, Binders, Efficiency, Burning Rate, Illumination		
20. ABSTRACT *(Continue on reverse side if necessary and identify by block number)* See back of form.		

DD FORM 1 JAN 73 1473 EDITION OF 1 NOV 65 IS OBSOLETE
S/N 0102-014-6601

UNCLASSIFIED
SECURITY CLASSIFICATION OF THIS PAGE *(When Data Entered)*

(U) *Physicochemical Details at the Surface of Burning Illumination Flares*, by J. L. Eisel and D. E. Zurn. China Lake, Calif., Naval Weapons Center, April 1975. 16 pp. (NWC TP 5726, publication UNCLASSIFIED.)

(U) The surface processes during the combustion of magnesium/sodium nitrate/binder illumination flares were observed using color cinephotomicrography. Examination of the films has led to several conclusions relative to the physicochemical details of pyrotechnic combustion of a limited class of materials. In binder-containing flares the surface temperature has been inferred at between 380°C and 651°C. The major means of removal of magnesium from the surface is expulsion in the condensed phase as a result of local overpressure due to interfacial oxidation and subsequent gasification of molten binder. The effect on intensity, efficiency and burning rate of magnesium particle size and content was examined, as well as of binder type and content. When little or no binder is present completely different processes dominate and surface temperatures are much higher.

INTRODUCTION

The surface processes which take place during the burning of magnesium/sodium nitrate/binder flares are extremely heterogeneous.[1,2] Without knowledge of these processes the design of more efficient systems must remain an art and a trial and error process. Similarly, the mathematical modeling of flare combustion will be less accurate than desired.

These processes are sensitive to a wide variety of parameters, including fuel-to-oxidizer ratio, fuel (metal) particle size, binder type, and binder content. While the reactions yielding the visible radiation, which is the desired end product of such devices, take place in the gas phase well away from the regressing surface, the surface processes have a direct effect on that radiation.

EXPERIMENTAL ARRANGEMENT

Direct observation of the surface details of combustion was made using high-speed, color cinephotomicrography. Figure 1 represents the experimental configuration. A Redlake Laboratories Hycam camera was used at a framing rate of 4000 frames per second and a film image-to-object magnification of two. The film used was Kodak Ektachrome EF Film 7241 (Daylight). Illumination was provided by a focused 2500 watt xenon lamp.

The flare samples were 1/4-inch diameter by 3/8-inch-long pressed at 15,000 psi. Compositions used are tabulated in Table 1.

---

[1] Eisel, J. L. "Observation of Surface Details of Burning Mg/$NaNO_3$/Binder Flares," *Proceedings of Third International Pyrotechnic Seminar*, Denver Research Institute/University of Denver, Denver, Colorado, 21-25 August 1972, pp. 435-41.

[2] Eisel, J. L. and D. E. Zurn. "On the Physicochemical Details at the Surface of Burning Illumination Flares," *Thirteenth Aerospace Sciences Meeting*, American Institute of Aeronautics and Astronautics, Pasadena, CA, January 1975, AIAA Paper No. 75-248.

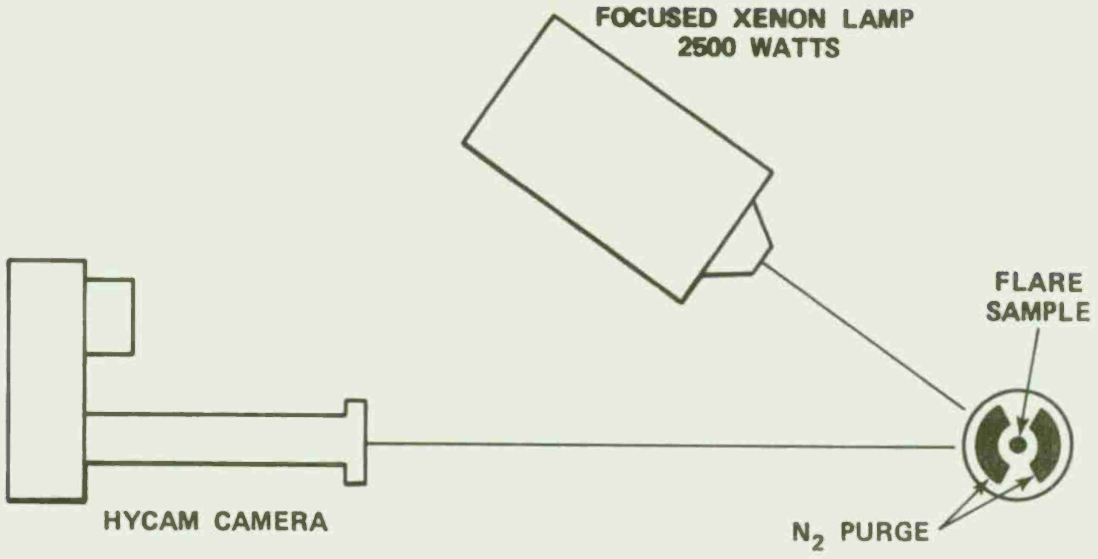

FIGURE 1. Test Configuration, Top View.

TABLE 1. Flare Compositions.

Designation	$NaNO_3$,[a] wt.%	Mg,[b] wt.%	Mg particle size, U. S. sieve	Viton A,[c] wt.%	Vitel,[d] wt.%
CT 257	26	70	60/70	4	
CT 258	41	55	60/70	4	
CT 259	56	40	60/70	4	
CT 260	35	55	60/70	10	
CT 261	41	55	120/140	4	
CT 262	26	70	60/70		4
CT 263	41	55	60/70		4
CT 264	56	40	60/70		4
CT 265	35	55	60/70		10
CT 266	41	55	120/140		4

[a] Davies Nitrate Co., Inc., Metuchen, N. J.
[b] Valley Metallurgical Co., Essex, Conn.
[c] Co-polymer of hexafluoropropylene and vinylidene fluoride.
[d] A polyester resin type PE-222.

All tests were conducted at atmospheric pressure (at China Lake one atmosphere ≈ 13.6 psia). Samples were burned vertically from the top with a flow of cold nitrogen passing upward from the base to carry combustion products

out of the camera field of view. Although the introduction of cold nitrogen drastically influences the radiation of the plume[3] the resultant degradation does not directly affect the processes at the surface. There is a decrease in energy feedback (relative to a larger diameter, unpurged flare) due to both the nitrogen and to the small flare diameter. However, these are constant losses and, therefore, do not result in relative changes at the surface. The burning rates and luminous intensities and efficiencies presented in Figures 4, 5, 6, and 12 were obtained using 7/8-inch-diameter by 1-inch-long samples. These data were obtained by the Pyrotechnics Branch, Code 4543, Naval Weapons Center. The nitrogen flow was not used in these tests.

OBSERVED DECOMPOSITION PROCESSES

For a typical magnesium/sodium nitrate/binder flare composition the observed surface behavior begins with the melting of the $NaNO_3$ and binder. Once melted, these two components become intimately mixed and cannot be visually observed as separate materials. Melting is followed by coalescence into globules of molten material. That is, the molten oxidizer/binder does not wet the receding flare surface, but rather draws up into isolated sites of material (Figure 2) which are capable of movement about on the surface. During steady combustion the surface temperature is such that

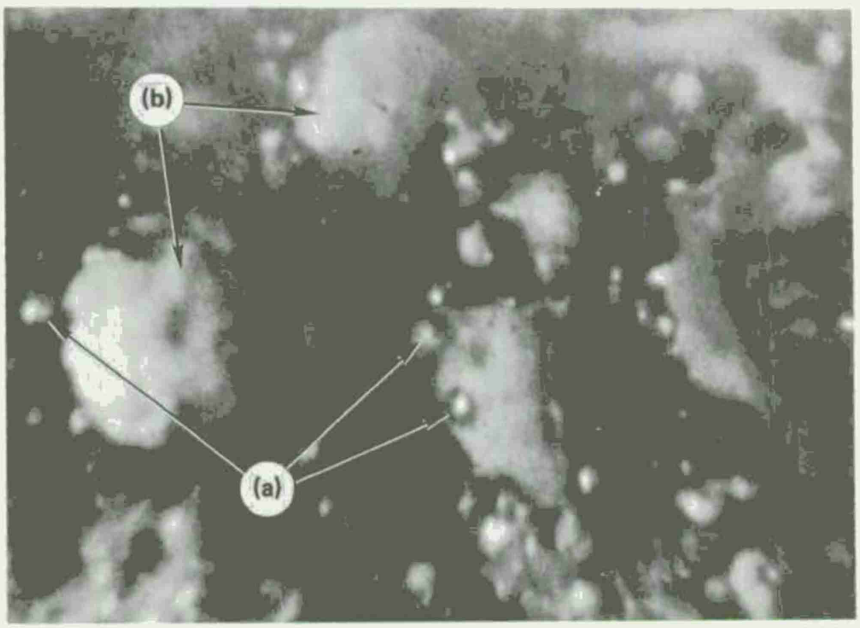

FIGURE 2. Burning Surface Structure of 55% Mg (200 μm)/41% $NaNO_3$/4% Viton A, (a) Magnesium Particles, (b) Oxidizer/Binder Globules.

[3] Dillehay, D. R. "Illuminant Performance in Inert Atmospheres," *Proceedings of Fourth International Pyrotechnic Seminar*, Denver Research Institute, 22-26 July 1974, pp. 2-1 to 2-14.

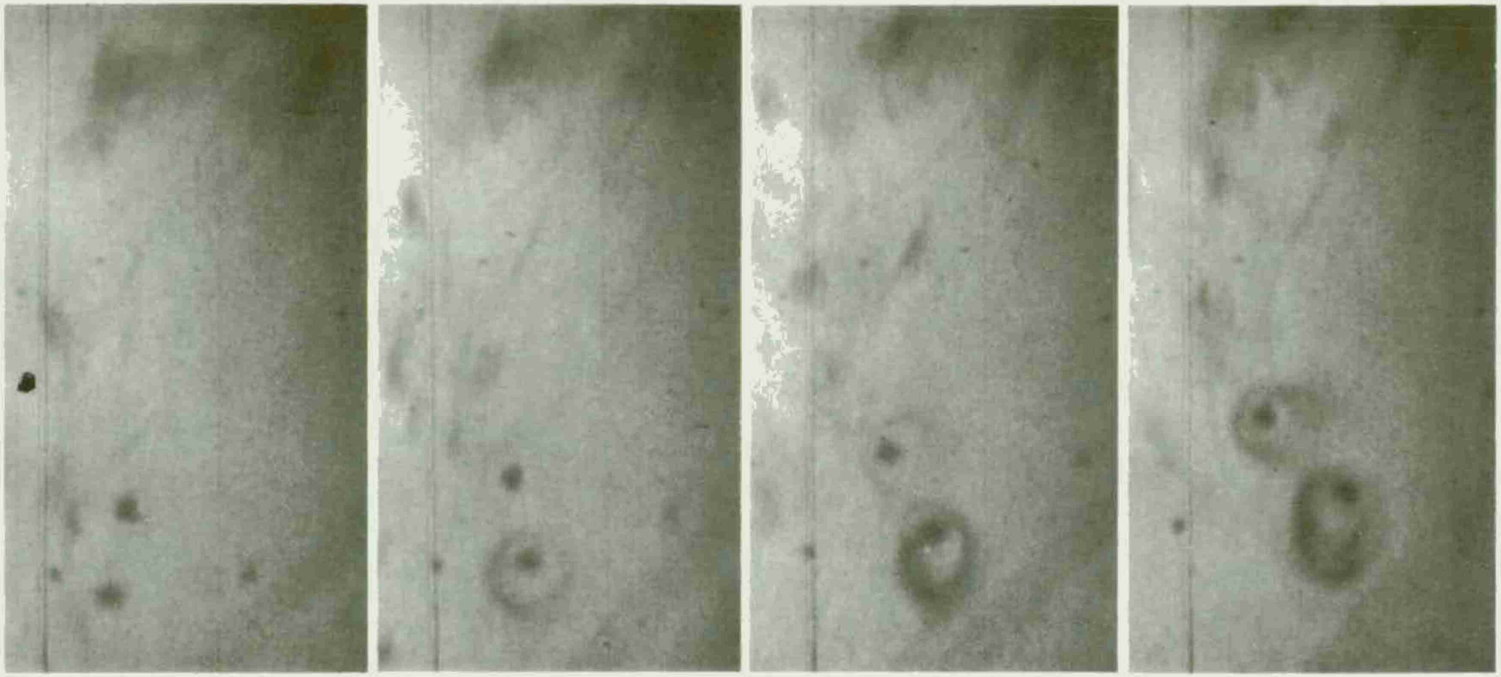

FIGURE 3. Ignition of Magnesium Particles About 1/2 Inch Above Burning Surface.

these globules actively decompose, probably giving off oxygen initially.[4] A given site remains identifiable throughout an extended period of the combustion and evolves from a basically white appearance to a red-brown and finally almost black color, possibly indicating an increase in the oxides of nitrogen. These decomposing globules range in size from less than 200 μm to nearly 1000 μm in diameter and in separation from one another over a similar range, depending on all of the variable parameters indicated earlier as influential on surface behavior.

Magnesium particles, upon exposure at the surface due to surface regression, can either be released and carried into the gas stream virtually unreacted or can be held at the surface and consumed, partially or *in toto*.

Particles leaving the surface unreacted were observed to kindle as much as 1/4 to 1/2 inch above the regressing surface. At that distance a dense cloud of MgO smoke was formed around the metal sphere, indicating rapid combustion (Figure 3).

It is far more common for the magnesium particles to be caught at the surface (Figure 2) on or within the decomposing oxidizer/binder globules. Once a particle is entrapped in such an oxidizing environment a surface oxidation process begins with the concomitant release of heat at the interface. When binder is present in the melt surrounding the magnesium particle, the local heat results in the gasification of the binder--also locally--and finally, in the production of a local overpressure. This imbalance of forces eventually results in the violent expulsion of the magnesium particle, not only from the engulfing globule, but also from the flare surface itself. Within two to five milliseconds prior to expulsion a magnesium particle not totally submerged in the oxidizing globule is seen to melt, as evidenced by a sudden wrinkling of the previously shiny surface. The expelled magnesium particle leaves at such a velocity that it cannot be time-resolved even at the high speed of the photographic observation. It appears the ejected particle is blown apart as one would expect of a liquid droplet subjected to such forces.

EFFECTS OF PARAMETER VARIATIONS

The magnesium content of the flares had a strong and monotonic effect on the burning rate of each of the flares tested (Figure 4) as well as on the average luminous intensity (Figure 5). But due to the commonly used definition of the efficiency of illumination flares the efficiency values obtained in this study are not quite so straightforward (Figure 6). Efficiency, as defined, can be viewed as the luminous intensity divided by the

[4] Bartos, H. R. and J.L. Margrove. "The Thermal Decomposition of $NaNO_3$," J PHYS CHEM, Vol. 60 (1956) p. 256.

mass burning rate. Thus, as seen in Figures 4, 5, and 6, although both the burning rate and the luminous intensity increase with increased magnesium content, the rate of increase of efficiency drops off with an actual decrease in efficiency for both binder-containing mixes. Such a loss in efficiency should not be viewed as unwanted, *per se*. The particular mission requirements must first be considered.

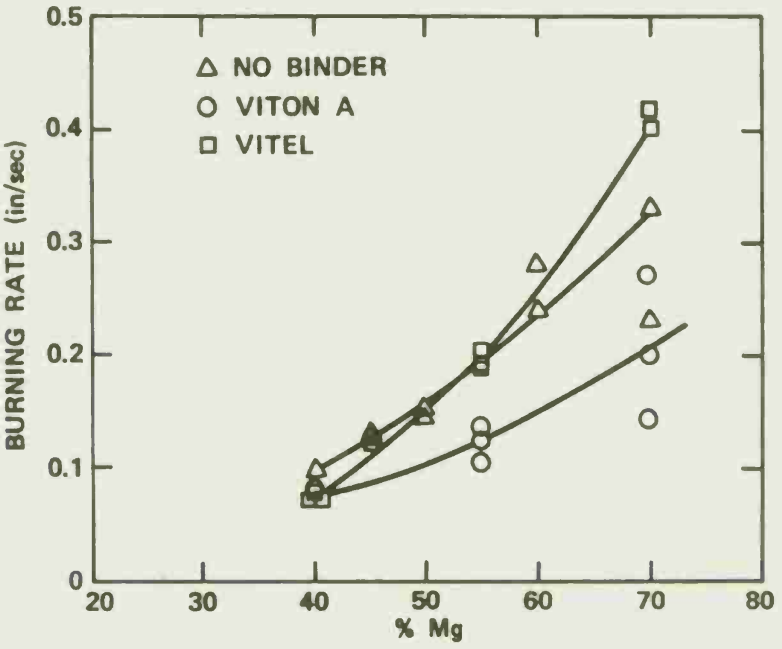

FIGURE 4. Burning Rates of Illumination Flare Mixes as a Function of Magnesium Content for 200 μm Magnesium.

Observation of the motion pictures of the systems studied indicated that as the magnesium content was increased the size of the oxidizer/binder globules decreased, their separation from one another decreased (Figure 7), and the overall surface activity increased. All of these effects reflect the increased burning rate accompanying the increases in metal fuel content.

When the diameter of the magnesium was decreased by a factor of two from ~ 200 μm to ~ 100 μm, the effects were significant, but not adequately consistent to draw firm conclusions. Table 2 shows the effects for 55/41/4 mixes of both Viton A and Vitel binders. For Viton A the average burning rate was increased 44 percent and the average luminous intensity was up 61 percent with the result that the efficiency was also up 16 percent. On the other hand, when the binder was Vitel, the average burning rate was up by 162 percent, but the average luminous intensity was down about seven percent, with a 65 percent loss in efficiency. Insufficient data were obtained to explain these results.

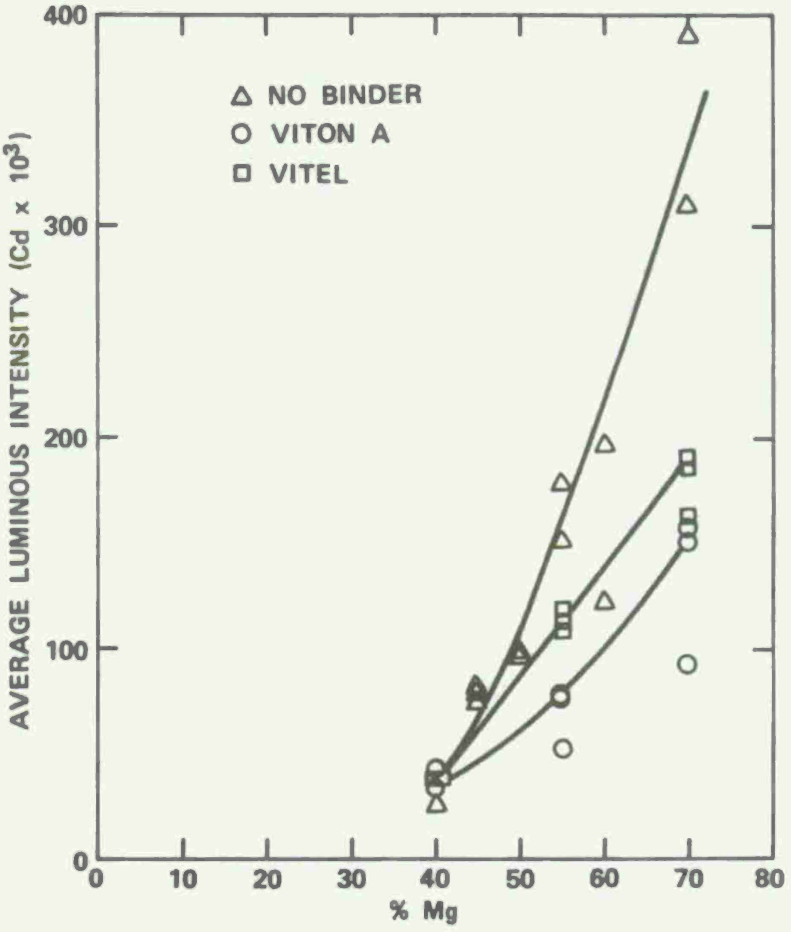

FIGURE 5. Average Luminous Intensity of Illumination Flare Mixes as a Function of Magnesium Content for 200 μm Magnesium.

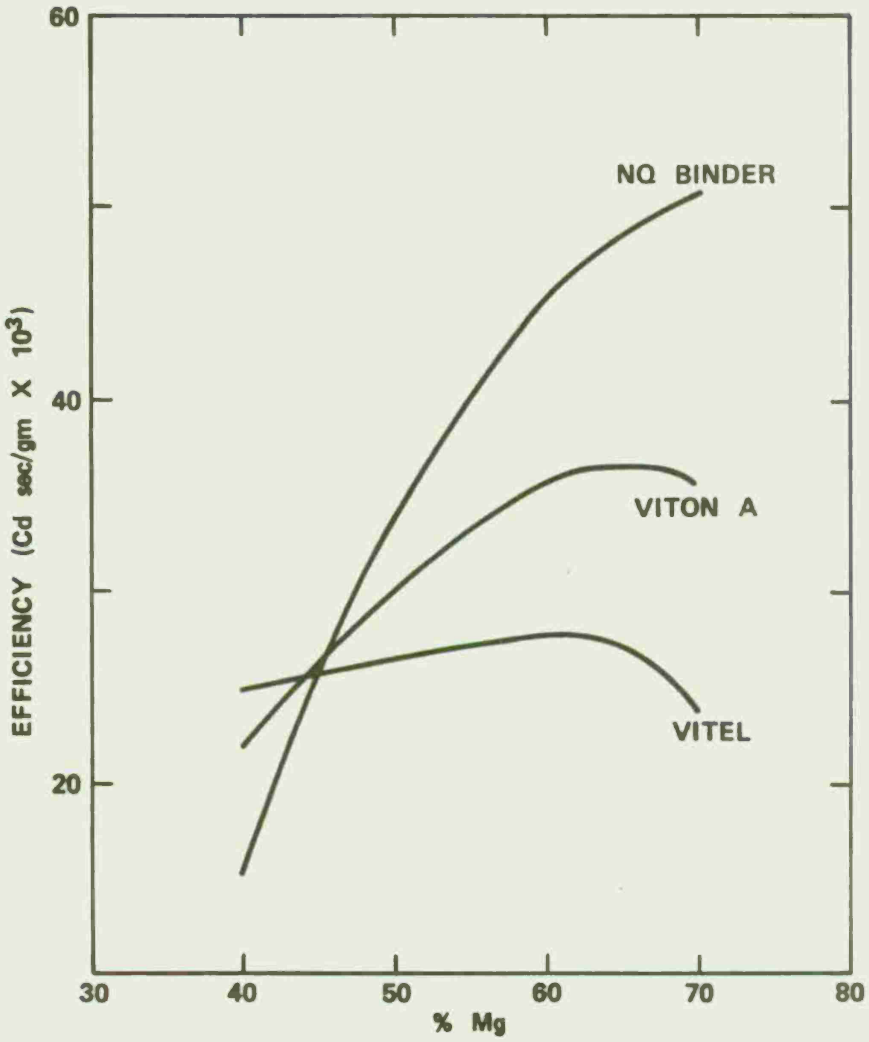

FIGURE 6. Efficiency of Illumination Flare Mixes as a Function of Magnesium Content for 200 μm Magnesium. Calculated from smoothed curves of Figures 4 and 5.

TABLE 2. Effect of Magnesium Particle Size.[a]

Binder	Approx. Mg size, μm	Burning rate, in/sec	Av. lum. intensity, Cd	Efficiency, Cd sec/gm
Viton A	200	.12	69×10^3	37.4×10^3
	100	.17	111×10^3	42.0×10^3
Vitel	200	.19	113×10^3	41.9×10^3
	100	.50	105×10^3	14.4×10^3

[a] Each entry is the average of three tests. All compositions are identical in weight fractions of constituents: 55% Mg/41% $NaNO_3$/4% binder.

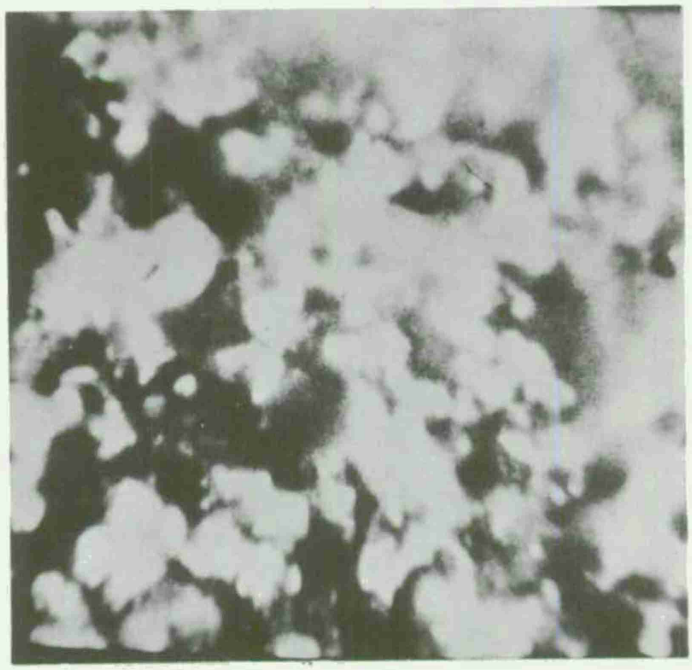

FIGURE 7. Burning Surface Structure of 70% Mg (200 μm)/26% $NaNO_3$/4% Viton A.

When the motion pictures were examined it was again observed, as with the increased metal content, that the oxidizer/binder globule size was greatly decreased (Figure 8) and the surface activity became even more intense. In addition, the main region of visible radiation was closer to the surface to the extent that viewing of the surface details became difficult due to over exposure of the film.

FIGURE 8. Burning Surface Structure of 55% Mg (100 μm)/41% $NaNO_3$/4% Viton A.

The differences observed for the two binders used in these series of tests were most apparent for four percent, or greater, binder content. The two binders were Viton A, a fluorocarbon, and Vitel, a polyester. At a given binder content the oxidizer/binder globules for the Viton A system were larger and less mobile than those of the Vitel system (Figures 2 and 9). The globules of the Viton A system tend to remain reasonably intact and in place upon the expulsion of a molten magnesium particle (Figure 10), re-forming into about the same volume as before. Upon expulsion of an engulfed particle from a Vitel-containing system the engulfing globule does not maintain its integrity, but rather disperses either into the gas stream or to other positions on the surface (Figure 11). The decomposing globules of the Vitel system tend to move about on the surface of the flare gathering up exposed magnesium particles and either expelling one or more of them or coming loose from the surface and carrying them away into the gas stream "plum pudding" fashion to continue to react and expel particles away from the surface. It appears, therefore, that the Viton A

system has higher surface tension and greater cohesion with the surface. In both cases newly exposed and melted oxidizer and binder, although sometimes forming new globules, most often are drawn into existing globules causing them to enlarge with time. The Vitel system seems to have a size threshold above which attachment to the surface is unlikely. In general, except at very low magnesium content, for a given magnesium loading the burning rate of the Vitel systems is higher (see Figure 4) than for the Viton A system. This may well reflect the endothermicity of the decomposing globules remaining at the surface in the Viton A system.

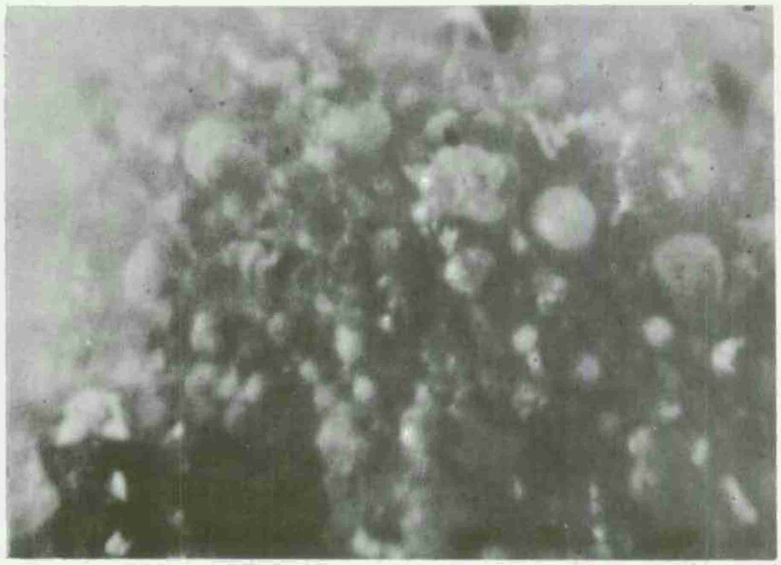

FIGURE 9. Burning Surface Structure of 55% Mg (200 μm)/41% $NaNO_3$/4% Vitel.

As the binder content was reduced to one percent or less in either of the systems, significant changes occurred. As seen in Figure 4, the burning rate of the binderless system was greater than that for the four percent Viton and approximately the same as that for the Vitel case. The average luminous intensity was significantly higher than for either four percent binder system (Figure 5). But, interestingly, both systems showed a peak in the intensity and efficiency curve in the region of one percent binder (Figure 12). This result is possibly due to the tendency for the binderless surface to break up and move into the gas stream prior to complete oxidation of the magnesium.

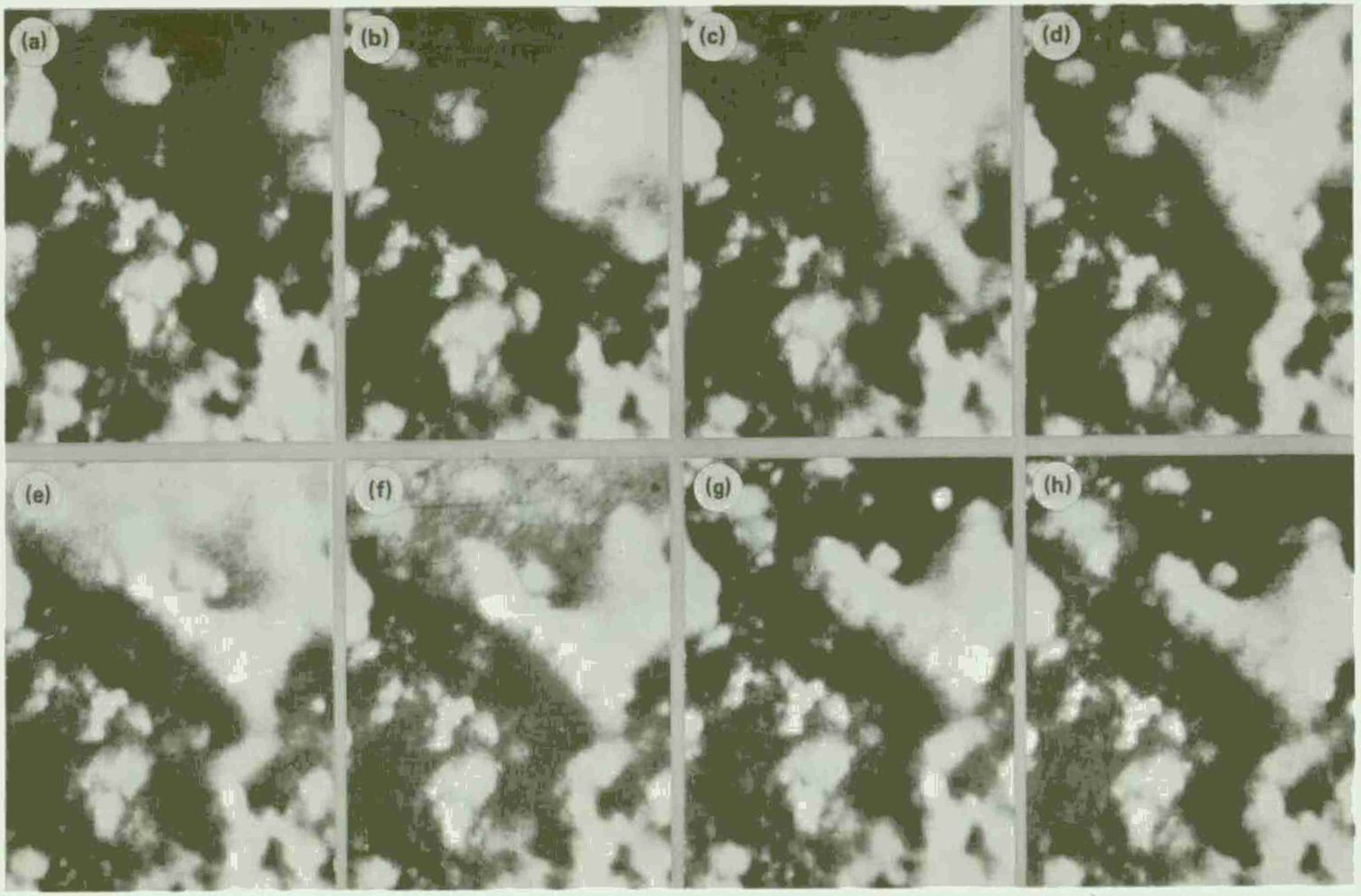

FIGURE 10. Series of Motion Picture Frames Showing Burning 55% Mg (200 μm)/41% $NaNO_3$/4% Viton A Flare Expelling Magnesium Particles From Oxidizer Globule. Note globule re-forms after particle leaves.

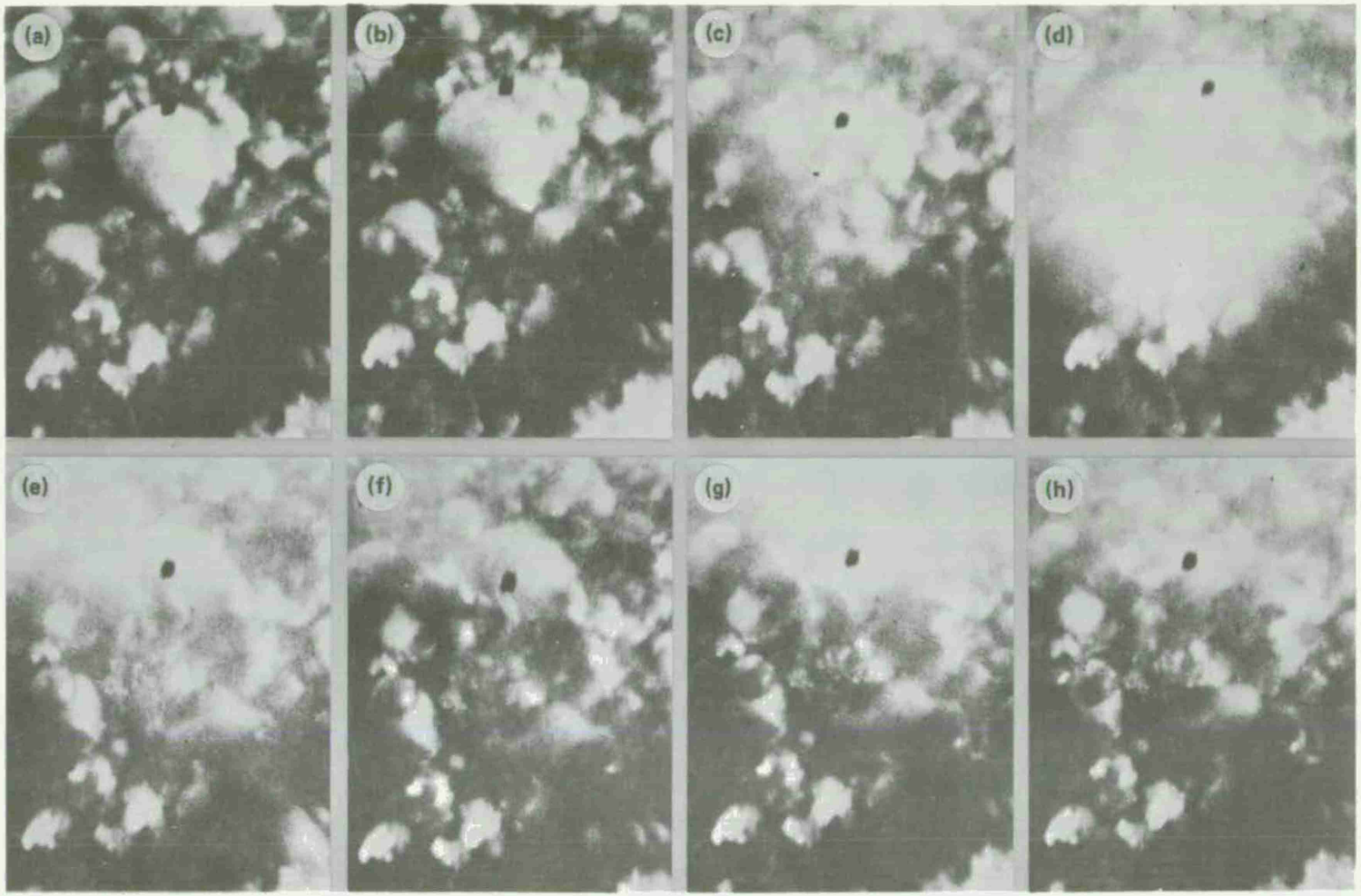

FIGURE 11. Series of Motion Picture Frames Showing Burning 55% Mg (200 μm)/41% $NaNO_3$/Vitel Flare Expelling Magnesium Particle From Oxidizer Globule. Note globule is completely dispersed after particle leaves.

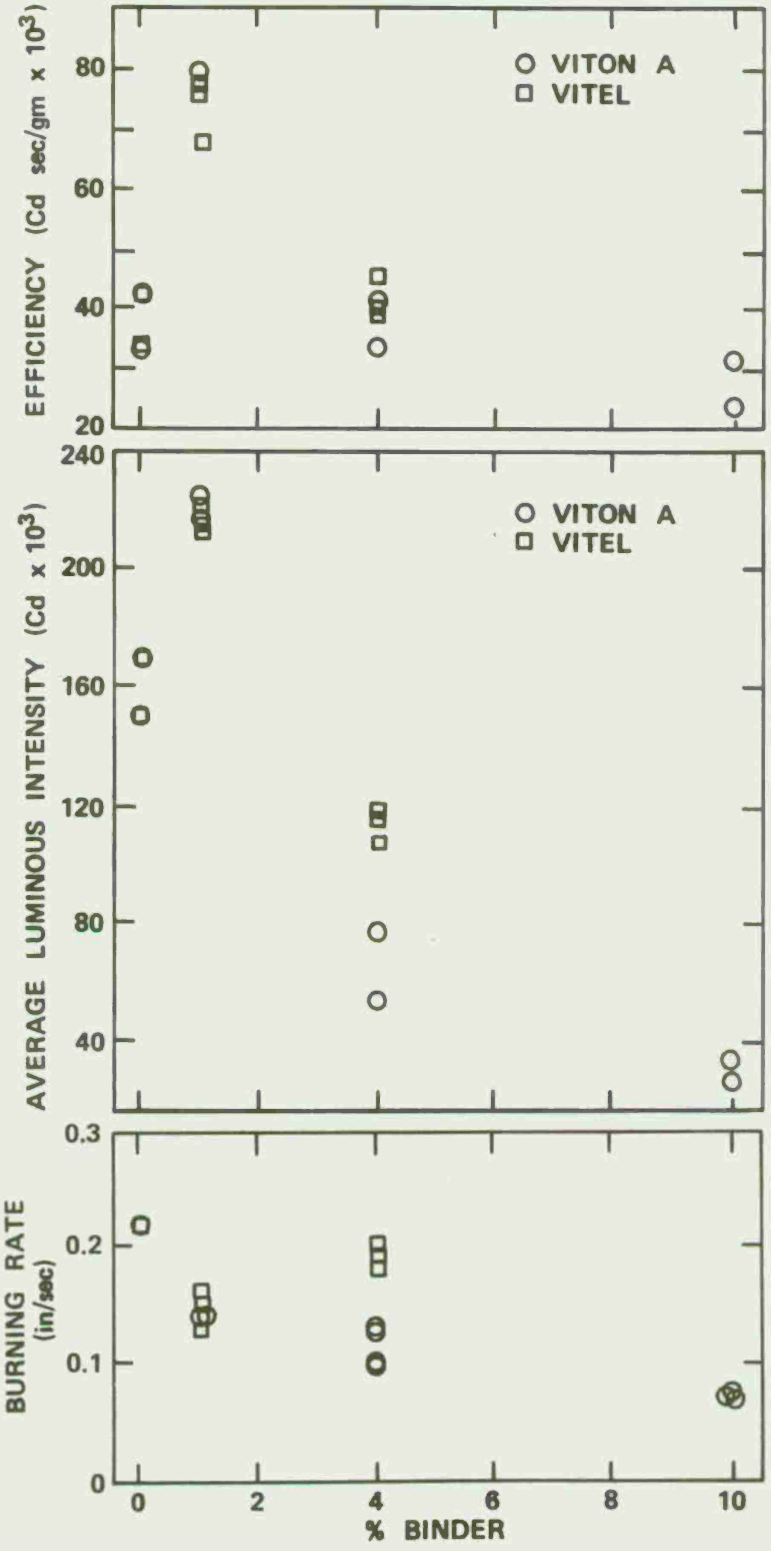

FIGURE 12. Performance of Illumination Flare Mixes Containing 55% Mg (200 μm) as a Function of Binder Type and Content.

In terms of surface observations these systems exhibited an entirely different type of behavior than those previously described containing one percent or less binder. Rather than expel engulfed magnesium the systems now retained the metal. Surface oxidation again took place, but since insufficient gasifying binder was present no overpressure existed and the particle remained and continued to oxidize. The surface oxide was seen to grow to cover an increasing portion of the metal surface and also to thicken (Figure 13). Usually this process continued until all of the metal had been either oxidized or vaporized, at which time the MgO crust became useless slag to remain on the surface as debris or to be carried away in the gas stream. The significant result of this process was that the amount of heat released at the flare surface was increased as was the efficiency of the transfer of heat to the surface. The result was the greatly enhanced burning rate. Since the radiating region of the flame was not studied, the reason for the increased radiation remains speculative although the higher mass efflux and the presentation of pre-vaporized metal to the oxidizing influence of the atmospheric air must be significant factors.

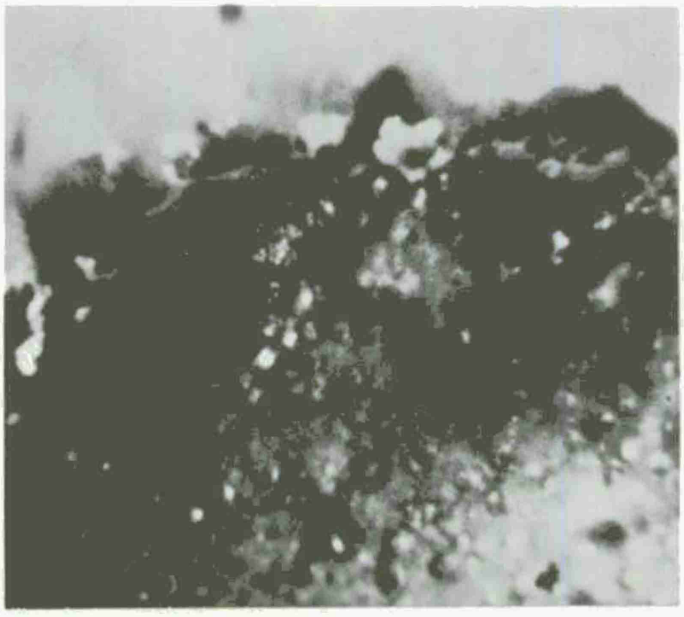

FIGURE 13. Burning Surface Structure of 55% Mg (200 μm)/44% $NaNO_3$/1% Viton A. Note molten surface and MgO "petal" left after oxidation and vaporization of Magnesium particle.

By noting that at binder content levels of four percent or greater significant MgO does not form at the surface, and by knowing[5] that the boiling decomposition of $NaNO_3$ begins at about 380°C and that magnesium melts at 651°C it is inferred that the surface temperature of such materials is within that range and varies over that range from place-to-place on the surface, with the exception of the immediate interfacial region where the heat released is sufficient to momentarily melt the magnesium particles. If, however, the binder content is reduced to a point where the magnesium is not expelled from the surface, the heat released by the prolonged oxidation reaction must increase the average surface temperature significantly.

SUMMARY AND CONCLUSIONS

It has been observed that the surface physicochemical processes of burning flares are extremely complex and certainly heterogeneous. The effect of increasing the metal content was seen to be more active surface conditions and visible radiation emitted closer to the surface resulting in increasing burning rates and luminous intensity, but a limit in the calculated efficiency was also seen. The effect of decreased metal particle size was seen also to result in increased burning rate and intensity and to bring the luminous radiation close to the surface. The effect of binder content was observed to have a significant effect on the mechanism and place of magnesium oxidation. When the binder content was as low as one percent the magnesium was no longer expelled molten into the flame zone, but was oxidized largely at the surface. The type of binder was not found to have large effects, only one of degree.

To say that one could now, or even eventually, design a universal flare is to be presumptive in the extreme. It remains a necessity to tailor a flare composition to its intended use. However, knowledge of the processes at the burning surface which manifest themselves ultimately as luminous output, burning rate and efficiency makes the design of flares for specific use a less artful and more controllable endeavor. Further research is necessary before precise flare design will be a possibility.

---

[5] Weast, R. C., ed. *Handbook of Chemistry and Physics*, 46th ed. Cleveland, Ohio, Chemical Rubber Co., 1966.

INITIAL DISTRIBUTION

16 Naval Air Systems Command
- AIR-310C (1)
- AIR-350 (2)
- AIR-350B (1)
- AIR-50174 (2)
- AIR-5102 (1)
- AIR-5108B (1)
- AIR-532D (1)
- AIR-53221 (3)
- AIR-5323 (1)
- AIR 53362 (2)
- AIR-5351 (1)

1 Chief of Naval Operations (OP-982)

2 Chief of Naval Material
- PM-20 (1)
- MAT-03426 (1)

7 Naval Sea Systems Command
- SEA-0332 (1)
- SEA-09B4 (4)
- SEA-09G32 (2)

1 Commandant of the Marine Corps (AAW-3B)

1 Marine Corps Development and Education Command, Quantico

2 Air Test and Evaluation Squadron 5

1 Fleet Composite Operations Readiness Group 2

2 Naval Air Development Center, Johnsville
- AMXP-4 (1)

9 Naval Ammunition Depot, Crane
- Code 20 (1)
- Code 50 (2)
- Code 50P (1)
- Code 503 (1)
- Code 504 (1)
- Code 506 (1)
- R&D Library (2)

1 Naval Ammunition Depot, Hawthorne (Code 05, Robert Dempsey)

1 Naval Explosive Ordnance Disposal Facility, Indian Head

1 Naval Material Data Systems Group, Morgantown

3 Naval Missile Center, Point Mugu
- Code 523 (1)
- Code 531 (1)

1 Naval Ordnance Station, Indian Head (Technical Library)

5 Naval Research Laboratory
  Code 4021R (3)
  Code 5117 (1)
  Code 7741 (1)
1 Naval Ship Engineering Center, Hyattsville (Code 6176C)
4 Naval Surface Weapons Center, White Oak
  Code 233 (2)
  Code 5 (1)
  Technical Library (1)
1 Naval Undersea Center, San Diego (Code 133)
4 Army Armament Command, Rock Island
  AMSAR-MTC, G. Cowan (1)
  AMSAR-SF (1)
1 Army Electronics Command, Fort Monmouth (Electronics Warfare Laboratory AMSEL-WL-N)
3 Edgewood Arsenal
  SMUEA-DE-MM (2)
  WDEL-GM Laboratory (1)
1 Frankford Arsenal (J1000)
1 Harry Diamond Laboratories (Technical Laboratory)
8 Picatinny Arsenal
  SARPA-VLI, Pyrotechnic Laboratory (3)
  SMD, Concepts Branch (4)
1 Air Force Systems Command, Andrews Air Force Base (DLPF)
3 Ogden Air Materiel Area, Hill Air Force Base
  OONEV (1)
  OOYE (1)
2 Aeronautical Systems Division, Wright-Patterson Air Force Base
  ASD/ENADC (1)
  ASD/RWEY (1)
3 Air Force Armament Laboratory, Eglin Air Force Base
  DLIP (1)
  DLO (1)
  AFAL/WRDZ (1)
1 Air Force Rocket Propulsion Laboratory, Edwards Air Force Base (Plans and Program Office)
1 Air Force Special Communications Center, San Antonio (SUR)
12 Defense Documentation Center
1 Explosives Safety Board (GB-270)
2 National Security Agency (Code 5232)

NWC 1290 C 805 4/75) 200